Pure & Appl. Chem., Vol. 66, No. 1, pp. 35–41, 1994.
Printed in Great Britain.

Structure and function of related proton channel-forming proteins

M.A. Harrison, P.C. Jones, Y-I. Kim, A. Holzenburg[1], M. E. Finbow [2] and J. B. C. Findlay

Dept. of Biochemistry and Molecular Biology and [1]Dep.artment of Genetics, University of Leeds, UK. and [2]Beatson Institute for Cancer Research, Glasgow, UK

Abstract

A molecular model has been constructed for a 16 kDa integral membrane protein which is the principal component of gap junction-like structures in the arthropod *Nephrops norvegicus*. This proteolipid is a member of a family of highly conserved proteins comprising the proton channel-forming subunits of vacuolar membrane (V-type) ATPases. The model suggests that the polypeptide exists as a transmembrane four-helical bundle, which assembles as a hexamer to form the membrane-spanning channel. The arthropod protein has been cloned and subsequently expressed in yeast, in which it complements a mutation in the endogenous gene for the related vacuolar membrane ATPase channel-forming subunit. Mutagenesis studies have been initiated in the yeast system in order to validate the structural model and to examine ion selectivity and transport mechanisms.

The regulated movement of ions through transmembrane channels is fundamental to a variety of processes, including cell-cell communication, signal transduction and homeostatic control. The great range of vital functions performed by ion channels consequently makes this a particularly important group of proteins. Crucial to understanding the essential mechanisms by which ions are transported across the lipid bilayer is an appreciation of relationships between structure and function in these ion channel proteins. Unfortunately, the strongly hydrophobic nature of integral membrane proteins introduces specific problems with regard to their isolation, purification and crystallisation, rendering the task of obtaining structural information particularly difficult. Significant advances have however been made in the area of membrane protein structure by combining the technique of high resolution electron microscopy with those of computergraphic modelling and structural prediction, classical protein chemistry and physical chemistry analyses. The application of these complementary techniques has provided detailed structures for integral membrane proteins for which high-resolution crystal structures are as yet not available (refs. 1,2).

We have applied the complementary techniques outlined above to the study of a 16 kDa, highly hydrophobic protein isolated from an arthropod (refs. 3, 4), but representative of a widespread and highly conserved family of proteins forming the putative proton channel component of an endomembrane-bound ATPase present in a variety of eukaryotic cell types (ref. 5). Current models suggest that the organisation of this ATPase complex is reminiscent of that proposed for the well-characterised F-type ATP synthases of chloroplasts and mitochondria, comprising a catalytic headgroup and a membrane channel sector (refs. 6, 7). However, these vacuolar membrane, or V-type, ATPases are distinctive in that they function exclusively as proton pumps driven by the hydrolysis of ATP, acting to acidify the interior of several intracellular organelles, including (but not restricted to) plant and fungal vacuoles, lysosomes, clathrin-coated vesicles and synaptic vesicles (for review, see ref. 6). In plants and fungi the proton motive force generated by the V-ATPase is utilised in the transport of a variety of ions into the vacuole, and the V-ATPase function is therefore essential for ionic homeostasis within the cell. The polypeptide has been implicated in the synaptic release of cytosolic acetylcholine from the mediatophore in response to calcium influx (ref. 8), and V-ATPase activity may be a prerequisite for dissociation of internalised receptor-ligand complexes.

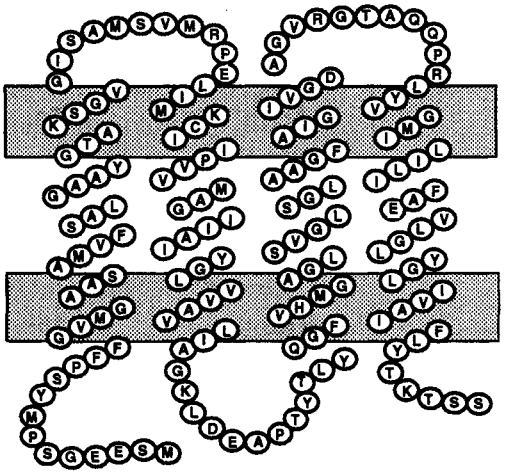

Fig.1: Disposition of the *Nephrops* 16 kDa protein within the bilayer based on secondary structure prediction and protein chemistry studies. Both termini are located to the inner (cytoplasmic) surface of the membrane.

The 16 kDa polypeptide from the hepatopancreas of the arthropod *Nephrops norvegicus* is isolated in homogeneous form as a paracrystalline paired membrane array which, under the electron microscope, is strongly reminiscent of the gap junctions of higher animals (ref. 3, 9, 10). The primary structure of the polypeptide has been determined by amino acid and cDNA sequencing, and shows a striking similarity to those of the proteolipid 16 kDa subunits of V-ATPases (ref. 3). Secondary structure predictions based on the sequence data, coupled with protease digestion and antibody binding studies, has allowed the construction of a model of the disposition of the protein in the lipid bilayer (Fig. 1). The polypeptide is proposed to be arranged as a bundle of four α-helices arranged sequentially in an anti-parallel orientation; the N-terminus is accessible to proteases in the *Nephrops* paracrystalline material, suggesting that it is the short extramembranous loops which interact to form the paired membrane structure. The four-helical bundle model is supported by FTIR data which indicate that approximately 65% of the total protein is α-helix (ref. 4).

The strong conservation of primary structure between 16 kDa polypeptide species is illustrated in Fig.2, which shows amino acid sequence alignments for 16 kDa polypeptides from diverse sources. Significant variation in sequence is seen only at the N-terminus and in the loop between the proposed helices 2 and 3. The hydrophobic regions forming each helix are almost universally conserved.

```
                    Helix 1                          Helix 2
Ne       MSEEGSPMYSPFFGVMGAASAMVFSALGAAYGTAKSGVGISAMSVMRPELIMKCIIPVVMAGIIAIYGLVVAVLIAGK
Dr    MSSEVSSDN-I-G----------II-------------T--A----------S---------------------A
Bo      MSEAKNG-E-AS--A----SA----------------T--A--------M---S--------------------NS
Mo      MADIKNN-E--S-------S-----------------T--A----------S--------------------NS
Sc3       MTELC-V-A---AAI-CSA-II-TS-------------C-TC-L--D-LF-N----------------S--VCYS
Sc11 MSTQLASNIY-L-A----FA-C-A---L-C----I------I--AGIGTFK------SL-----S---------------N

                    Helix 3                          Helix 4
Ne  LDEAPT*YTLYQGFVHMGAGLSVGLSGLAAGGAIGIVGDAGVRGTAQQPRLYVGMILILIFAEVLGLYGLIVAIFLYTKTSS
Dr  -E-PSK*-S--R--I-L----A--F-----------------------F--------------------Y----
Bo  -NDGIS***--RS-LQL-----------------------------F--------------------LI-S--
Mo  -TDGIT***---S-LQL-----------------------------F--------------------LIIST-
Sc3 -GQKQA***--T--IQL-------------------------SS-----F--------------------LL-NSRATQDVV
Sc11-SPTED*---FN--M-LSC--C--FAC-SS-Y---M---V---KYMH----F--IV-----S-------M---LI-N-RG-E
```

Fig. 2. Sequence alignments for related 16 kDa proton channel proteins. N-terminal regions (upper panel) and C-terminal regions (lower) have the positions of proposed transmembrane helices indicated. Dashes indicate conserved residues. Asterisks indicate spaces inserted to optimise alignment. Ne.; *Nephrops* (ref. 3). Dr.; Drosophila (ref. 14). Bo.; Bovine chromaffin granule (ref. 15). Mo.; Murine (ref. 16). Sc3.; *Saccharomyces* VMA3 gene product (ref. 17). Sc11.; *Saccharomyces* VMA11 gene product (ref. 18).

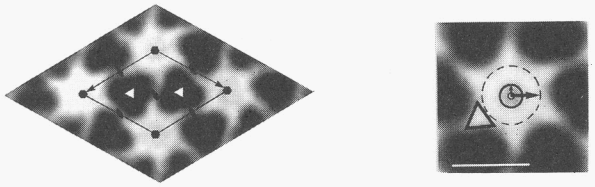

Fig. 3. High-resolution electron microscopy of *Nephrops* gap junction-like structures. [Left panel] Reconstructed projection of the unit cell after optical filtering and rotational averaging over two centres of three-fold symmetry. In negative stain protein appears white. Centres of 2-, 3- and 6-fold symmetry are indicated. [Right panel] Reconstructed projection of a single hexameric complex after optical filtering and 6-fold rotational averaging. The central mass deficit (small arrow) has a radius of 0.75 nm, and the radius of the outer ring is 1.9 nm from the centre of the complex (large arrow). The marked triangular protrusions cover an area of 1.6 nm^2. Scale bar is 5 nm. Reproduced from Holzenburg et al. (1993), European Journal of Biochemistry (in press)

The same is true of the 1-2 and 3-4 extramembranous loops, indicating conservation of the regions of the polypeptide which are in contact with catalytic subunits of the diverse V-ATPases.

High-resolution electron microscopy of negatively-stained paracrystalline arrays from *Nephrops* and subsequent projection averaging shows the macromolecular structure of the gap junction-like array to comprise hexamers of approximately 7.5 nm diameter, with a stain-penetrable pore of 1.5 nm at the centre (ref. 4). Examples of the images obtained by this method are shown in Fig. 3, in which the hexameric assembly of the gap junction unit is clearly defined. Estimations of molecular volume from the averaged projections provide an estimated mass for the hexamer of 110 kDa, clearly consistent with a macromolecular organisation requiring six 16 kDa polypeptides. This is consistent with stoichiometry studies which also indicated six copies of the 16 kDa proteolipid in each Vo channel complex (ref. 11).

Combining the electron microscopy data with analysis by structural prediction and hydrophobicity moment algorithms (refs. 12, 13), along with protein chemistry data, has permitted the construction of a detailed macromolecular model in which six copies of the four-helical bundle 16 kDa protein associate to form a channel which is structurally and functionally analogous to the Fo channel of the ATP synthases. The computergraphic model of the hexamer is shown in Fig.4. Interestingly, the 16 kDa polypeptide shares sequence similarity with the 8 kDa subunit c of the Fo channel, and is a tandem repeat of that protein (ref. 15), twelve copies of which are thought to be incorporated into the Fo channel.

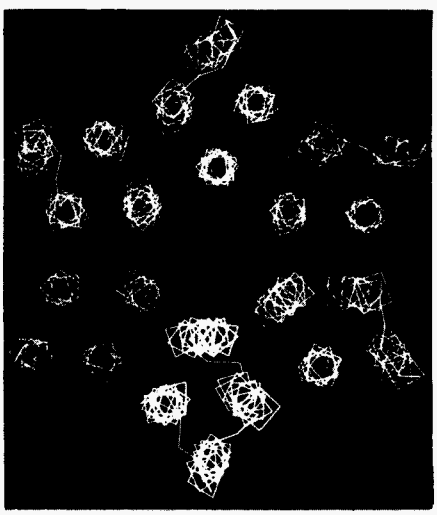

Fig.4. Computergraphic model for the hexameric array of *Nephrops* 16 kDa polypeptides. Helix 1 lines the pore of the channel, with helices 2, 3 and 4 arranged in a clockwise orientation.

The relative disposition of the four helices of the 16 kDa protein, based on the crystallographic structure of a four-helical bundle (ref. 19), is shown in Fig. 5: three of the four faces of helices 2 and 4 are hydrophobic, whereas only one face of helix 3, and none of helix 1 show strong hydrophobicity. Two opposite faces of helix 3 are rich in glycine and alanine residues, with the remaining face showing a number of polar residues (Ser99 and Ser103, for example). In common with helix 3, helix 1 shows opposing faces enriched in glycine and alanine, the remaining two faces being enriched in polar or charged residues. Orientation of helix 3 furthest from the putative central pore of the hexamer, with its single polar face directed into the four-helical bundle, presents a continuous hydrophobic surface to the lipid milieu which is of sufficient length to pass through the bilayer (indicated as white regions in Fig. 5). Several polar or charged residues are positioned to the interior of the four-helical bundle, including the essential DCCD-reactive Glu140 residue (refs. 20, 28, 31), which occurs on the otherwise exclusively hydrophobic helix 4, and a conserved lysine residue (Lys35) of helix 1. The only discontinuity in the hydrophobic surface of the four-helical bundle is the outer face of helix 1, which contains Thr33 and a strip of small polar residues, a pattern of amino acids proposed to line the pores of ion channels (ref. 21). Constraints imposed by molecular mechanical considerations are imposed on the model, and helices are arranged such that crossover of extramembranous loops is minimised, as occurs in other four-helical bundles.

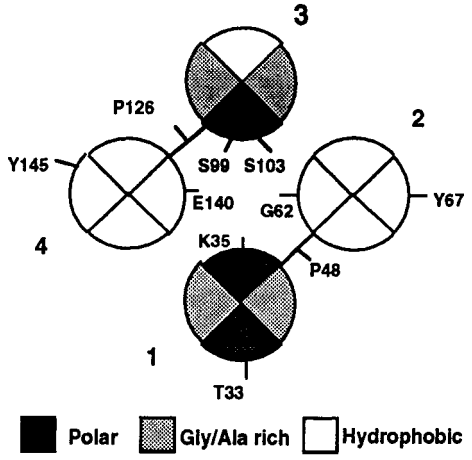

Fig. 5. Predicted orientation of the four-helical bundle of the 16 kDa *Nephrops* protein. Helix 1 is proposed to be proximal to the central channel of the hexameric array.

In order to test and validate the working model for the four-helical bundle of the 16 kDa and the hexameric channel into which it is assembled, a system which is amenable to mutagenesis and in which the protein is accessible to protein chemistry studies, is required. We have recently demonstrated the expression of the *Nephrops* 16 kDa protein in a yeast system in which the endogenous VMA3 gene, encoding the equivalent 16 kDa subunit of the Vo channel of the yeast vacuolar membrane ATPase (see Fig. 2), has been disrupted (ref. 22). In the absence of a functional V-ATPase, the yeast cell is unable to grow at pH 7.5 and is unable to tolerate high concentrations of exogenous Ca^{2+} ions (ref. 23). Complementation with the *Nephrops* gene restores growth at the otherwise lethal pH 7.5. We have subsequently isolated the hybrid V-ATPase from yeast cells and shown that it is functionally equivalent to the wild type enzyme in terms of activity, subunit composition and inhibitor sensitivity (manuscript in preparation). It is clear therefore that the arthropod 16 kDa protein substitutes functionally for the yeast protein. Expression in yeast therefore represents a suitable system in which to experimentally test the predictions of the 16 kDa model.

Questions arise concerning the relationship between ion selectivity and structure and function of the 16 kDa protein. Recent evidence suggests that the Vo channel of the vacuolar membrane is closed to protons in the absence of the V_1 catalytic headgroups (refs. 24, 25). Is it interaction with V_1 (as in the case of the V-ATPase) which keeps the hexameric channel open? Is ion selectivity conferred solely by the catalytic headgroup of the V-ATPase, or are additional components of the Vo channel involved? Furthermore, is the pathway of proton translocation through the central pore of the hexamer or through the four-helical bundle? It should be possible to address these questions by observing ion transport properties *in vitro* using purified and reconstituted 16 kDa protein containing

amino acid residues modified by site-directed mutagenesis. To facilitate isolation, we have used PCR-based mutagenesis to introduce a C-terminal polyhistidine domain into the *Nephrops* protein. This group of six histidyl residues has high affinity for Ni^{2+} ions at high pH. The detergent solubilized protein can be isolated by affinity chromatography on an immobilised Ni^{2+}-NTA agarose matrix (refs. 26, 27).

TABLE 1. Functional properties of *Saccharomyces* strains expressing the *Nephrops* 16 kDa protein. Vacuolar membrane ATPase specific activities are expressed as μmol ATP hydrolysed/mg protein/min. Km is expressed for ATP (mM). Vacuolar membrane isolation and ATPase assay were performed essentially as in ref 28.

Strain	V-ATPase Specific activity	Km
Wild type	0.21	0.2
VMA3⁻	None	-
Nephrops 16 k	0.21	0.4
*Neph.*16 k (Hisx6)	0.31	1.8

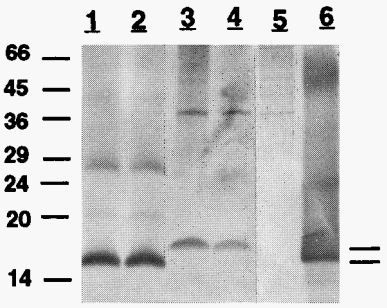

Fig. 6. Immunoblot detection of *Nephrops* 16 kDa protein expression in *Saccharomyces cerevisiae.* Vacuolar membrane proteins were analysed by SDS-polyacrylamide gel electrophoresis, blotted and probed with polyclonal antisera to the arthropod gap junction complex. The VMA3⁻ strain was transformed with the *Nephrops* 16 kDa as follows: [1] native *Nephrops* gene. [2] C54S strain (see text for details). [3, 4] *Nephrops* gene with C-terminal polyhistidine. [5] non-transformed VMA3⁻ [6] Gap junction protein sample.

Table 1 lists the functional V-ATPase activities in purified vacuolar membranes from VMA3⁻ yeast strains expressing the *Nephrops* 16 kDa polypeptide, with or without the polyhistidine group. Complementation of the VMA3⁻ mutation with the arthropod gene restore V-ATPase activity to wild type levels, but the activity has a somewhat higher Km for ATP. This Km is further increased when the 16 kDa protein contains the polyhistidine affinity group. These data suggest that although the *Nephrops* protein substitutes functionally for the native yeast VMA3 gene product even when modified by the addition of six histidine residues, minor changes to the structure of the Vo channel have significant repercussion at the ATP-binding site of the V-ATPase, resulting in measurable disfunction. The immunoblot of vacuolar membrane protein shown in Fig. 6 illustrates the expression of the *Nephrops* protein in yeast. Total vacuolar membrane proteins were probed with polyclonal antibodies raised against the gap junction-like material from the arthropod hepatopancreas. Note the immunoblot development corresponding to the expressed *Nephrops* protein in yeast, and its absence in membranes of the VMA3⁻ strain. Note also that the protein modified by the addition of the polyhistidine group shows an expected greater molecular mass than the native 16 kDa protein. We have successfully used the Ni^{2+} affinity chromatography procedure to isolate detergent-solubilized 16 kDa polypeptide from yeast vacuolar membranes in a form suitable for reconstitution experiments (manuscript in preparation).

A strategy which has successfully been used to determine the relative positions of individual amino acid residues within a protein involves the introduction of cysteine residues at specific sites (refs. 29, 30). These sites are subsequently probed with hydophilic or hydrophobic cysteine-specific modifying reagents, enabling discrimination between residues adjacent to the lipid phase or adjacent to an aqueous environment. To test the structural model for the 16 kDa protein, in particular with respect to the position of helix 1, we have replaced individual residues with cysteines through a complete α-helical turn of helix 1. Residues 24-27 and 29-31 have been modified in this way, in a cysteine-free mutant protein engineered by mutating the single cysteine residue at position 54 of the native *Nephrops* protein to a serine residue (see Fig. 2). Control substitutions at residues 6 and 44 have also been created.

These residues should be outside the transmembrane domain and should be freely accessible to hydrophilic reagents.

In advance of protein labelling studies, we have made functional measurements of vacuolar membrane ATPase activity in the complement of cysteine substitution mutants (Table 2). The activity of the V-ATPase in the cysteine-free mutant (C54S) was approximately 80% of that in the strain expressing the native *Nephrops* protein, but with unaltered Km for ATP. These strains also grew at the same rates under the selective pH conditions. Cysteine substitutions at residues 6, 26, 27, 29, 30 and 44 did not significantly alter V-ATPase activity , Km for ATP or growth rate at pH 7.5, suggesting little overall influence on the structure of the Vo proton channel. However, introduction of cysteine residues at positions 24 and 25 gave greatly reduced growth rates under selective conditions, increased V-ATPase specific activity in the vacuolar membrane (measured at non-physiological ATP concentration) and a correspondingly higher Km for ATP. Introduction of a cysteine residue at position 31 also greatly reduced growth at pH 7.5.

TABLE 2. Functional properties of *Saccharomyces* strains expressing the mutagenised *Nephrops* 16 kDa protein. Codes refer to the changed residue, its position in the primary structure and the amino acid which has been introduced. Vacuolar membrane ATPase specific activities are expressed asμmolATP hydrolysed/mg protein/min. Km is expressed for ATP (mM). Vacuolar membrane isolation and ATPase assay were performed as in ref. 28. Values in parentheses reflect ATPase activity relative to that in the C54S mutant. ND, not determined.

Mutant strain	Specific activity	Km	Growth at pH 7.5
C54S	0.17 (100)	0.4	+
S6C	0.12 (71)	0.4	+
F24C	0.29 (171)	0.7	+/-
S25C	0.29 (171)	0.8	+/-
A26C	0.13 (76)	0.4	+
L27C	0.16 (94)	0.4	+
A29C	0.12 (71)	0.4	+
A30C	0.17 (100)	0.4	+
Y31C	ND	ND	+/-
S44C	0.15 (88)	0.4	+

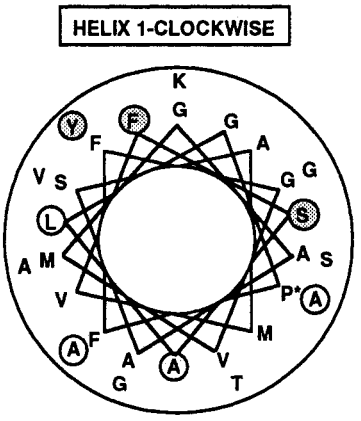

Sequence:

PFFGVMGAASAMV FSALGAAY GTAKSGV

Fig. 7. Helical wheel projection for helix 1 of the *Nephrops* 16 kDa protein. The α-helix runs clockwise and starts at the indicated proline residue. The region of the helix in which cysteine substitutions have been made is underlined and indicated in the figure by circles. Shaded circles indicated substitutions causing ATPase disfunction.

The Km data suggest that introduction of cysteine residues to positions 24, 25 and 31 reduce V-ATPase activity at physiological ATP concentration, and that the cell compensates by assembling more copies of the hybrid ATPase, reflected as higher specific activity for V-ATPase under *in vitro* assay conditions. These data become more illuminating when the projected positions of the altered residues within helix 1 are considered. Figure 7 shows a schematic helical wheel projection for helix 1 of the 16 kDa protein. The helix is arranged such that the Lys35 residue, proposed to face into the four-helical bundle, is to the top and the putative pore-lining residues are to the bottom (as for Fig. 5). The amino acid residues which have individually been changed to cysteine residues are ringed, with those alterations which give rise to V-ATPase disfunction shaded. A clustering of residues is immediately obvious, with residues affecting ATPase function sited on the face of the helix proposed to be oriented into the centre of the four-helical bundle.

These data, although preliminary, may already provide clues towards understanding the pathway of proton movement in the V-ATPase: it seems clear that amino acid residues lining the centre of the helical bundle are more critical than those lining the central channel. This in turn is consistent with the absolute conservation of charged residues Glu140 (Fig. 2) and Lys35 (ref. 31), which must also face into the four-helical bundle. It is also consistent with the well-documented observation that proton translocation is strongly inhibited by modification of Glu140 by DCCD. A plausible

mechanism for proton translocation through the four-helical bundle might involve protonation/deprotonation of Glu140, and would be facilitated by the presence of ATP-hydrolysing V_1 subunits. This mechanism would be analogous to that proposed to involve acidic residues in bacteriorhodopsin (ref. 1), and would not be precluded by the tight packing of the four-helical bundle. It should be possible in the near future to resolve these issues and to refine the structural and functional models by studying ion transport properties of the reconstituted and mutagenised 16 kDa protein *in vitro*.

REFERENCES

1. R. Henderson, J. M. Baldwin, T. A. Ceska, F. Zemlin, E. Beckmann and K. H. Downing *J. Mol. Biol.*,**218**: 899-929 (1990).
2. W. Kuhlbrandt and D. N. Wang *Nature*, **350**: 130-134 (1991).
3. M. E. Finbow, E. E. Eliopoulous, P. J. Jackson, J. N. Keen, L. Meagher, P. Thompson, P. C. Jones and J. B. C. Findlay *Protein Engineering*, **5**: 7-15 (1992).
4. A. Holzenburg, P. C. Jones, T. Franklin, T. Pali, T. Heimburg, D. Marsh, J. B. C. Findlay and M. E. Finbow *Eur. J. Biochem.*, in press (1993).
5. N. Nelson *Trends Pharmacol. Sci.*, **12**: 71-75 (1991).
6. N. Nelson *Curr. Opin. Cell Biol.* **4**: 654-660 (1992).
7. Y. Anraku, N. Umemoto, R. Hirata and Y. Wada *J. Bioenerg. Biomembr.*, **21**: 589-603 (1989).
8. S. Birmans, F.-M. Meunier, B. Lesbats, J.-P. Le Caer, J. Rossier and M. Israel *FEBS Lett.*, **261**: 303-306 (1990).
9. M. E. Finbow, T. E. J. Buultjens, N. J. Lane, J. Shuttleworth and J. D. Pitts *EMBO J.* **3**: 2271-2278 (1984).
10. B. Leitch and M. E. Finbow *Exp. Cell Res.*, **190**: 218-226 (1990).
11. H. Arai, G. Terres, S. Pink and M. Forgac *J. Biol. Chem.*, **263**: 8796-8802 (1988).
12. E. E. Eliopoulous, A. J. Geddes, M. Brett, D. J. C. Pappin and J. B. C. Findlay *Int. J. Biol. Macromol.*, **4**: 263-268 (1982).
13. F. Jahnig *Trends Biochem. Sci.*, **15**: 93-95 (1990).
14. L. Meagher, P. McLean and M. E. Finbow *Nucleic Acids Res.*, **18**: 6712 (1990).
15. M. Mandel, Y. Moriyama, J. B. Hulmes, Y.-C. E. Pan, H. Nelson and N. Nelson *Proc. Natl. Acad. Sci. USA* **85**: 5521-5524 (1988).
16. H. Hanada, M. Hasebe, Y. Moriyama, M. Maeda and M. Futai *Biochem. Biophys. Res. Commun.*, **176**: 1602-1607 (1991).
17. H. Nelson and N. Nelson *FEBS Lett.*, **247**: 147-153 (1989).
18. N. Umemoto, Y. Ohya and Y. Anraku *J. Biol. Chem.*, **266**: 24526-24532 (1991).
19. C. Cohen and D. A. D. Parry *Proteins.* **7**: 1-15 (1990).
20. S. Z. Sun, X. S. Xie and D. K. Stone *J. Biol. Chem.*, **262**: 14790-14794 (1987).
21. N. Unwin *Neuron*, **3**: 665-676 (1989).
22. H. Nelson and N. Nelson *Proc. Natl. Acad. Sci. USA* **87**: 8503-8507 (1990).
23. Y. Ohya, N. Umemoto, I. Tanada, A. Ohta, H. Iida and Y. Anraku *J. Biol. Chem.* **266**: 13971-13977 (1991).
24. J. Zhang, M. Myers and M. Forgac *J. Biol. Chem.*, **267**: 9773-9778 (1992).
25. C. Béltran and N. Nelson *Acta Physiol. Scand.*, **146**: 41-47 (1992).
26. E. Hochuli, W. Bannwarth, H. Dobeli, R. Gentz and D. Stuber *Bio/Technology*, **6**: 1321-1325 (1988).
27. R. Janknecht, G. de Martynoff, J. Lou, R. A. Hipskind, A. Nordheim and H. G. Stunneberg *Proc. Natl. Acad. Sci. USA* **88**: 8972-8976 (1991).
28. E. Uchida, Y. Ohsumi and Y. Anraku *J. Biol. Chem.*, **260**: 1090-1095 (1985).
29. C. Altenbach, T. Marti, H. G. Khorana and W. L. Hubbell *Science*, **248**: 1088-1092 (1990).
30. M. Akabas, D. A. Stauffer, M. Xu and H. Karlin *Science*,**258**: 307-310 (1992).
31. T. Noumi, C. Bèltran, H. Nelson and N. Nelson *Proc. Natl. Acad. Sci. USA*, **88**: 1938-1942 (1991).